Journal of Materials Chemistry C

ROYAL SOCIETY OF CHEMISTRY

PAPER

View Article Online
View Journal

Cite this: DOI: 10.1039/d4tc03269a

Impact of steric effects on the statistical probability factor in triplet–triplet annihilation upconversion†

Lukas Naimovičius, Simon K. Zhang and Andrew B. Pun *

Received 31st July 2024,
Accepted 5th October 2024

DOI: 10.1039/d4tc03269a

rsc.li/materials-c

The statistical probability factor (*f*) in triplet–triplet annihilation (TTA) upconversion (UC) is one of the key elements governing UC performance. This factor indicates the probability that an emissive singlet state is generated upon two triplet states undergoing TTA. Therefore, UC quantum yield has a maximum value of *f*/2 if all other processes within the system approach unity. As an intrinsic property of annihilator compounds, the *f* value is thought to mostly depend on the annihilator's excited state energy level distribution. However, emerging results in the field of TTA-UC indicate that steric effects have a substantial influence on the *f* factor and UC performance. In this work, we demonstrate that the *f* factor is composed of both energetic and steric components. We study a series of energetically similar diketopyrrolopyrrole (DPP) annihilators. By modulating the various alkyl groups appended to the DPPs, we demonstrate a strategy to enhance the *f* factor, and therefore UC performance, by limiting steric interactions.

Introduction

Triplet–triplet annihilation (TTA) upconversion (UC) is a non-linear optical process that converts two low-energy photons into one of higher energy.[1–8] TTA-UC is of particular interest, compared to other UC mechanisms,[9] due to its high efficiency under incoherent low energy density excitation.[10–14] This leads to various applications including photovoltaics, photocatalysis, 3-D printing, and biosensing.[4,15–24] TTA-UC systems are composed of two species, sensitizers and annihilators. The sensitizer is responsible for the absorption of low energy photons and generation of an excited triplet (T_1) species *via* intersystem crossing (ISC). The annihilator chromophores accumulate those triplets *via* collisional Dexter-type triplet energy transfer (TET) from the sensitizer. Two annihilators in their T_1 state can then meet and undergo TTA, resulting in an emissive excited singlet (S_1) state (Fig. 1a). TET and TTA occur at short distances (<10 Å) upon collision between sensitizer and annihilator, and two individual annihilators, respectively. The core-to-core collision between two annihilators is preferred for a more efficient triplet coupling due to triplet wavefunction localization on the conjugated core of the annihilator.[13,25,26] The TTA-UC quantum yield (Φ_{UC}) is defined as follows:

$$\Phi_{UC} = \frac{1}{2} f \Phi_{ISC} \Phi_{TET} \Phi_{TTA} \Phi_{PL} \quad (1)$$

where $\frac{1}{2}$ indicates one generated photon per two absorbed, f is the statistical probability factor, and Φ_{ISC}, Φ_{TET}, Φ_{TTA}, Φ_{PL} are the

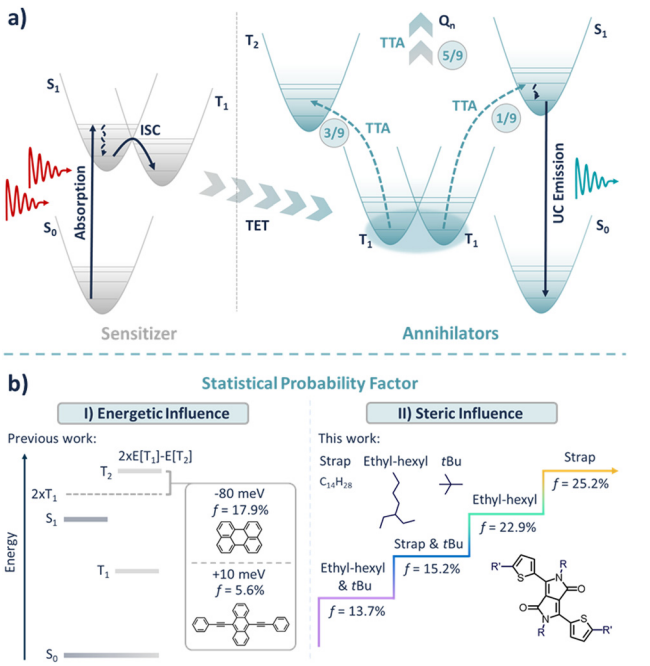

Fig. 1 (a) Scheme of TTA-UC indicating energy transfer processes of intersystem crossing (ISC), triplet energy transfer (TET), and triplet–triplet annihilation (TTA). (b) Components comprising the statistical probability factor *f* including (I) energetic influence (previous work),[27,28] and (II) steric influence (this work).

Department of Chemistry and Biochemistry, University of California San Diego, 92093 La Jolla, CA, USA. E-mail: abpun@ucsd.edu

† Electronic supplementary information (ESI) available. See DOI: https://doi.org/10.1039/d4tc03269a

quantum yields of sensitizer intersystem crossing, sensitizer to annihilator triplet energy transfer, triplet–triplet annihilation between two annihilators, and annihilator photoluminescence, respectively.

The *f* factor refers to the intrinsic probability of the generation of an emissive singlet state when two triplets meet and undergo TTA (Fig. 1a). This value is specific to every annihilator. The maximum Φ_{UC} is governed by the *f* value, with an intrinsic limit of $\Phi_{UC} = f/2$ if all other processes in eqn (1) approach unity efficiency. Therefore, the *f* factor is one of the most important benchmarks for direct comparison between annihilators and their potential UC performance.

According to the Clebsch–Gordan series, triplet coupling results in 9 spin-pair states with 1 singlet, 3 triplets, and 5 quintets corresponding to their multiplicities (Fig. 1a).[25,29–31] These statistics indicate the *f* value is limited to 1/9, but triplet (T_n) state recycling *via* internal conversion (IC) increases this limit to 2/5.[25,30] Additionally, in the case of weakly exchange-coupled triplet-pair states with parallel geometry, three states are of mixed singlet–quintet character, thus boosting the theoretical maximum *f* value to 2/3.[25] Conversely, the weakly exchange-coupled triplet-pair states with perpendicular geometry limit the *f* value to 2/5, thus highlighting the importance of the orientation factor.[25] Recently, annihilators surpassing the intrinsic limit of 2/5 were reported with *f* factors up to 54%.[6,28,32–36] It is believed that the distribution of excited state energy levels is the key component governing the *f* value.[6,25,27,30,37,38] The energy gap law was introduced as a potential cause limiting *f* factor due to the energy level distribution of the annihilator. The energy of the first excited state triplet ($E[T_1]$), second excited state triplet ($E[T_2]$) and first excited state singlet ($E[S_1]$) are most important. In particular, the differences in energy of $2 \times E[T_1]$–$E[T_2]$ and $2 \times E[T_1]$–$[S_1]$ impact TTA probability and non-radiative loss channels (Fig. 1b).[30,37–39] If $2 \times E[T_1]$ is closer to $E[T_2]$ than to $E[S_1]$, upon TTA, it is more likely that an annihilator T_2 state will form rather than its S_1 state due to the energy gap law. This T_2 state is non-emissive, which leads to a reduction of UC efficiency.

However, emerging patterns of the *f* value in the field of TTA-UC demonstrate that both energetic and steric effects have a substantial influence of UC performance.[30,36,40] In this work, we elucidate the impact of steric effects on the *f* factor by synthesizing diketopyrrolopyrrole (DPP) annihilators with similar excited state energy landscapes. These derivatives have different alkyl chains to demonstrate an approach to tune the *f* value solely by steric effects. This differs from previous work, where the addition of bulky groups to annihilators was used to reduce aggregation and excimer formation interfering with TTA.[7,41] In contrast to the annihilators used in these previous studies, our DPP annihilators do not exhibit aggregation or excimer formation, even at high concentrations (Fig. S3 and S6, ESI†). *f* values for these different DPPs range from 13.7% up to 25.2%, as bulky alkyl groups are removed. As the excited state energy level distributions remain similar in our DPPs, steric effects are the main reason for the increasing *f* value. Therefore, we show a generalized synthetic approach to optimize annihilator performance *via* functionalization with alkyl moieties.

Results and discussion

Theoretical approach

Prior to experimental characterization, we performed time-dependent density functional theory (TD-DFT) calculations and molecular dynamics (MD) simulations to show the intrinsic differences between our DPP compounds (Fig. 2). The DFT calculations indicated minimal variation of $E[T_1]$ between DPP compounds (1.23–1.26 eV) (Fig. 2). Similar minor fluctuation from 2.71 eV to 2.79 eV (Fig. 2) was seen for $E[S_1]$. These fluctuations in $E[S_1]$ matched experimental trends (Fig. 3a)

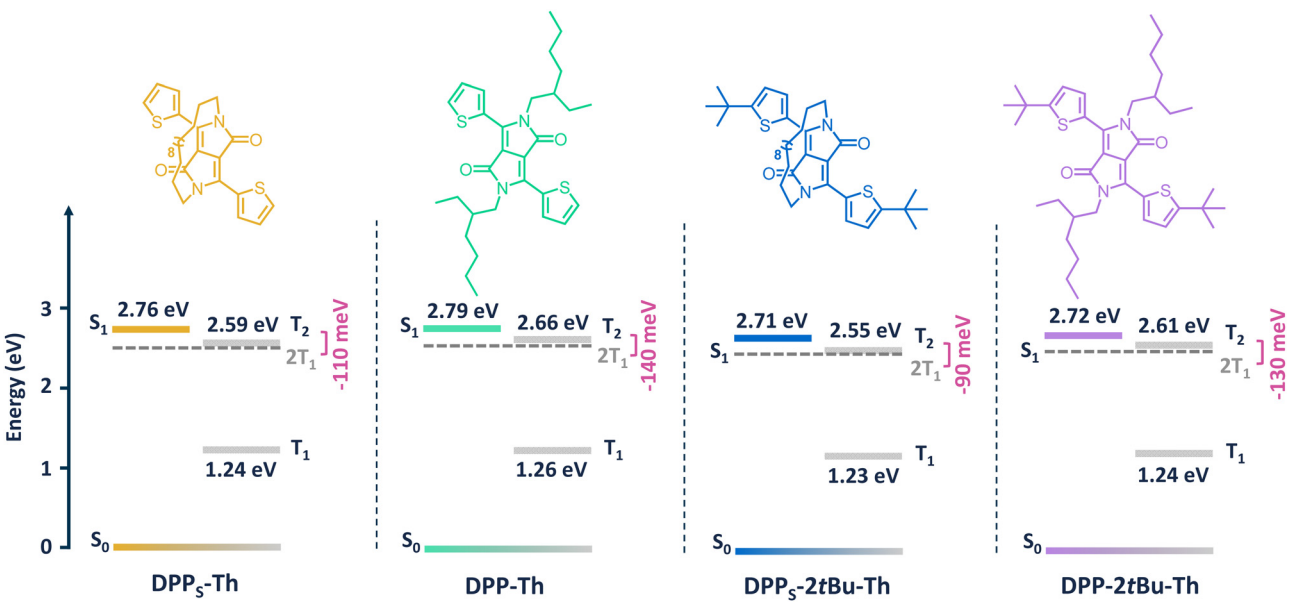

Fig. 2 Chemical structures of the studied DPP annihilators and calculated triplet (T_1, T_2) and singlet (S_1) excited energy states of DPP compounds. $2 \times E[T_1]$–$E[T_2]$ indicated in pink.

despite being overestimated by 0.5 eV. This overestimation of $E[S_1]$ for DPP compounds has been previously reported.[40] In general, the excited state energy level distributions of our DPPs remained similar across the studied compounds with the $2 \times E[T_1]$–$E[T_2]$ energy gap fluctuating in a range between −90 meV to −140 meV (Fig. 2, pink). The similarity in excited state energies between our annihilators allowed us to isolate the influence of steric interactions on the *f* value.

Following energy level distribution calculations, steric effects were theoretically investigated with MD simulations. These were focused on two main factors that may have a substantial influence on the *f* value: (i) plane-to-plane intermolecular distance between the DPP cores during the collision between two annihilators; (ii) strain angle of the DPP annihilator core during the collision.

The plane-to-plane distance between the cores governs TTA probability due to the non-radiative Dexter-type energy transfer mechanism occurring at a distance below 10 Å. The wavefunction overlap between the annihilators during intermolecular coupling was shown to possess an optimal distance for TTA.[26] A smaller plane-to-plane distance implies optimized TET and TTA, leading to more efficient UC. According to annihilator collision simulations, the strapped compounds (**DPP$_S$-Th** and **DPP$_S$-2*t*Bu-Th**) have a smaller average core-to-core distance (3.65 Å) compared to unstrapped counterparts **DPP-Th** (4.85 Å) and **DPP-2*t*Bu-Th** (4.97 Å) (Fig. S1a and b, ESI†). The difference indicates that an annihilator with a strapped alkyl chain is likely to have higher rates of TET and TTA as compared to an annihilator with conventional unstrapped alkyl chains, such as the ethyl-hexyl groups we use here. Compared to strapped moieties, bulkier ethyl-hexyl side chains limit how close two annihilators can be to one another (Fig. S1b, ESI†). As the ethyl-hexyl groups are flexible, neither side of the annihilator core is exposed during the collision, limiting both TTA and TET rates. Interestingly, the *t*Bu functionalization demonstrated a negative effect on intermolecular distance. This may be explained by additional steric effects due to bulky *t*Bu moieties which inhibit annihilators from approaching one another.

The core strain angle representing the bending of an annihilator core relative to the main axis was also estimated (Fig. S2, ESI†). The average core strain angle during the collision is slightly larger for *t*Bu functionalized compounds primarily due to additional intermolecular interactions. Strapped DPPs also demonstrated an increase in strain angle compared to unstrapped annihilators. Usually, larger strain values lead to higher photoluminescence quantum yields (Φ_{PL}) in DPP annihilators.[40] Together, the theoretical calculations suggested that strapped annihilators with less bulky moieties are most likely to be efficient TTA-UC annihilators.

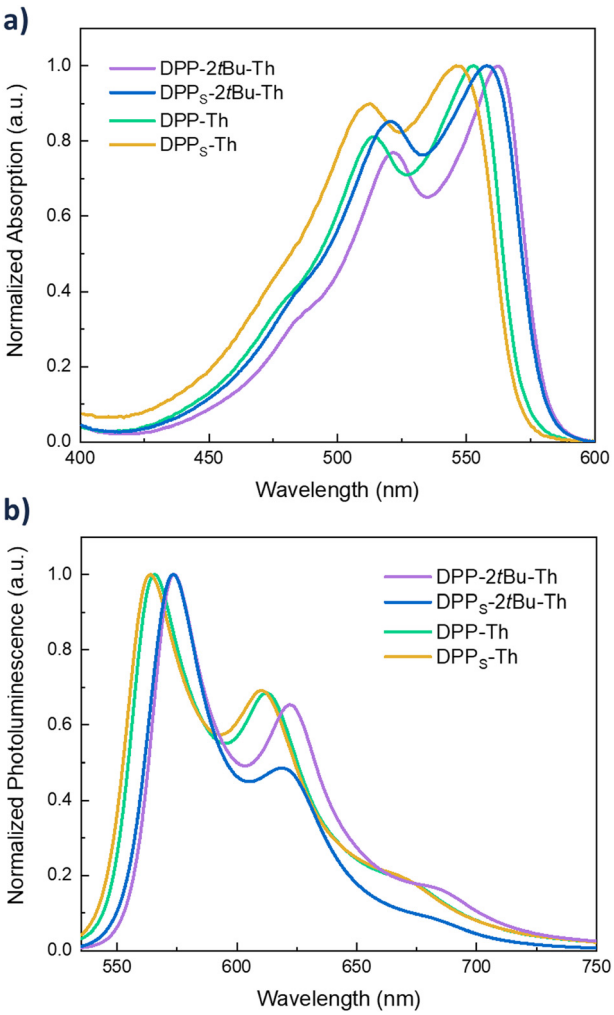

Fig. 3 (a) Normalized absorption of studied DPP compounds at 10^{-5} M concentration in toluene. (b) Normalized photoluminescence of studied DPP compounds at 10^{-5} M concentration in toluene.

Photophysical characterization

To begin experimental characterization, the absorption and emission spectra of our DPP compounds were investigated. The absorption of **DPP$_S$-Th**, **DPP-Th**, **DPP$_S$-2*t*Bu-Th**, and **DPP-2*t*Bu-Th** gave λ_{max} values of 546 nm, 553 nm, 558 nm and 563 nm, respectively (Fig. 3a). Small variations in the amplitude of the 0–1 vibronic peak were observed in the absorption and emission spectra of our studied compounds (Fig. 3a and b). These deviations are likely caused by core strain due to the presence of the strapped alkyl chain and/or the bulky *t*Bu groups which limit accessible vibrational levels. These small differences indicated similar energy level distributions for the studied compounds which were weakly affected by alkyl functionalization, matching our theoretical results (Fig. 2).

The photoluminescence quantum yields (Φ_{PL}) for **DPP$_S$-Th**, **DPP-Th**, **DPP$_S$-2*t*Bu-Th**, and **DPP-2*t*Bu-Th** in dilute solution (10^{-5} M in toluene) were 65%, 53%, 78%, and 70%, respectively (Table 1).

Triplet–triplet annihilation

To determine the *f* values for the studied DPP annihilators, solution state UC measurements were performed. From this, we could extract quantum yields of upconversion (Φ_{UC}), triplet energy transfer (Φ_{TET}), and triplet–triplet annihilation (Φ_{TTA}).

Table 1 Main parameters of the studied DPP compounds and DPP:PdPc UC solutions

Compound	Φ_{PL} [a] (%)	$\Phi_{UC,g}$ [b] (%)	$\Phi^{\infty}_{UC,g}$ [c] (%)	Φ_{TET} [d] (%)	I_{th} [e] (W cm^{-2})	f [f] (%)
DPP$_S$-Th	64.8	4.8	6.5	79.8	15.7	25.2
DPP-Th	52.7	3.5	4.6	76.4	16.7	22.9
DPP$_S$-2*t*Bu-Th	78.2	3.4	4.8	81.6	15.3	15.2
DPP-2*t*Bu-Th	69.9	3.1	3.4	69.8	6.8	13.7

[a] PL quantum yield in 10^{-5} M toluene solution. [b] Self-reabsorption corrected UC quantum yield. [c] Maximum achievable UC quantum yield at infinity I_{ex}. [d] TET quantum yield. [e] Threshold excitation intensity at 38.2% of the maximum achievable UC quantum yield. [f] Statistical probability factor calculated from eqn (1). UC systems measured with an annihilator concentration of 26 mM and sensitizer concentration of 30 μM in toluene.

The DPP annihilators were combined with a metalated macrocycle sensitizer, PdPc. This compound is known to have a T_1 energy of 1.24 eV,[42] sufficient to sensitize DPP.[40,43] Additionally, the ISC quantum yield (Φ_{ISC}) for PdPc was reported to approach unity.[42]

DPP:PdPc UC solutions were prepared by changing the annihilator concentration (1–26 mM) while PdPc concentration remained constant (30 μM). The Φ_{UC} values were determined *via* the relative quantum yield method reported elsewhere,[27,44–46] utilizing indocyanine green as a standard (Table S1, ESI†). The DPPs exhibited enhanced Φ_{UC} with increasing annihilator concentration (Fig. 4). The increase in Φ_{UC} over annihilator concentration is consistent with previous reports.[33,36,47,48]

The high annihilator concentrations (26 mM) utilized for the DPP:PdPc UC solutions led to detrimental self-reabsorption, diminishing Φ_{UC}. Self-reabsorption corrections were performed as previously reported by our group and others, *via* fitting of PL spectra over UC emission (Table S2 and Fig. S3, ESI†).[6,40,44–46] The method also allowed us to correct for the use of a 700 nm short-pass filter during the measurements to avoid the influence of a 730 nm laser excitation. The self-reabsorption corrected UC quantum yields ($\Phi_{UC,g}$) gave values of 4.8%, 3.5%, 3.4%, and 3.1% for **DPP$_S$-Th**, **DPP-Th**, **DPP$_S$-2*t*Bu-Th**, and **DPP-2*t*Bu-Th**, respectively (Table 1).

To avoid underestimation of the f value, the maximum achievable UC quantum yield ($\Phi^{\infty}_{UC,g}$) was evaluated by performing Φ_{UC} measurements as a function of excitation power density (I_{ex}) (Fig. S4, ESI†). The Φ_{UC} dependence on I_{ex} was fitted with the method proposed by Murakami *et al.*[49] allowing us to determine the UC threshold (I_{th}) as well as $\Phi^{\infty}_{UC,g}$ (Fig. S4, ESI†). As I_{ex} approaches infinity, another important TTA-UC parameter, the Φ_{TTA}, approaches unity, thus facilitating the f value estimation. I_{th} determined by this method is defined as the I_{ex} at 38.2% of $\Phi^{\infty}_{UC,g}$.[49] As I_{th} is important for the practical application of DPP annihilators in TTA-UC, we evaluated I_{th} for the studied DPP:PdPc UC solutions. I_{th} fell in the range between 6.8 W cm^{-2} to 16.7 W cm^{-2} (Table 1 and Fig. S4, ESI†). These values are high compared to other TTA-UC systems, but similar

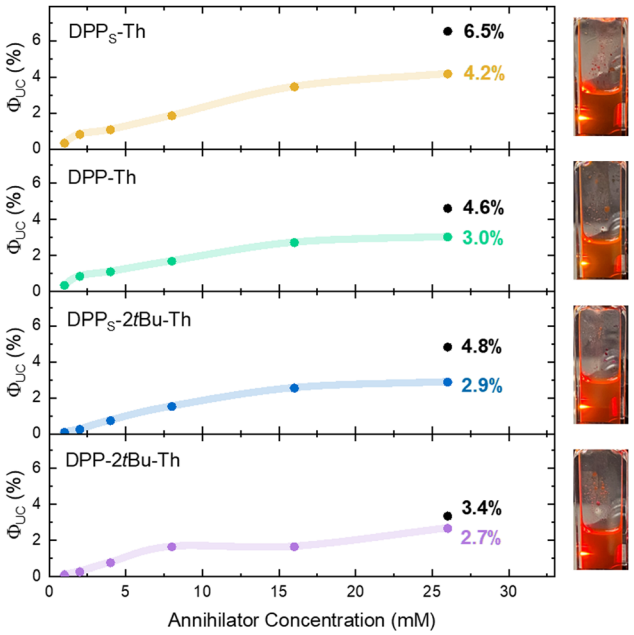

Fig. 4 Upconversion quantum yield (Φ_{UC}) dependence (dots) on annihilator concentration for the studied DPP:PdPc UC solutions in toluene. Line is shown as a guide for an eye. Black dots indicate the maximum achievable upconversion quantum yield ($\Phi^{\infty}_{UC,g}$) according to the method proposed by Murakami *et al.*[49] PdPc concentration was maintained at 30 μM for all measurements. Upconversion images depicted for each DPP:PdPc solution at 26 mM annihilator concentration under 730 nm laser excitation.

to previously reported TTA-UC systems utilizing DPPs as an annihilator.[40]

The strapped **DPP$_S$-Th** and **DPP$_S$-2*t*Bu-Th** demonstrated superior $\Phi^{\infty}_{UC,g}$ of 6.5% and 4.8%, respectively, compared to unstrapped **DPP-Th** (4.6%) and **DPP-2*t*Bu-Th** (3.4%) counterparts (Fig. 4 and Table 1).

As expected, the strap alkylation was favorable for higher $\Phi^{\infty}_{UC,g}$ mainly due to the enhanced Φ_{PL} and a slight increase in the Φ_{TET} discussed below. According to the results, the best-performing **DPP$_S$-Th** compound outperformed the widely used rubrene annihilator (5.6%)[36] emitting in the same range showing the potential of functionalized DPP compounds for efficient TTA-UC. By optimizing the DPP:PdPc UC systems, we also demonstrate the most efficient DPP annihilator reported in the literature.[40,43]

To continue the investigation of our DPP:PdPc UC systems, we conducted Φ_{TET} measurements *via* Stern–Volmer quenching experiments (Fig. S5, ESI†). Φ_{TET} was evaluated as follows:

$$\Phi_{TET} = 1 - \frac{\Phi_{P(UC)}}{\Phi_P} \quad (2)$$

where $\Phi_{P(UC)}$ is the phosphorescence quantum yield of the sensitizer in DPP:PdPc UC solution, and Φ_P is the phosphorescence quantum yield of the sensitizer in the absence of annihilator, which has been previously shown to be 77%.[50] $\Phi_{P(UC)}$ and Φ_P correspond to the integrated intensity of quenched (I) and unquenched (I_0) sensitizer phosphorescence, respectively.

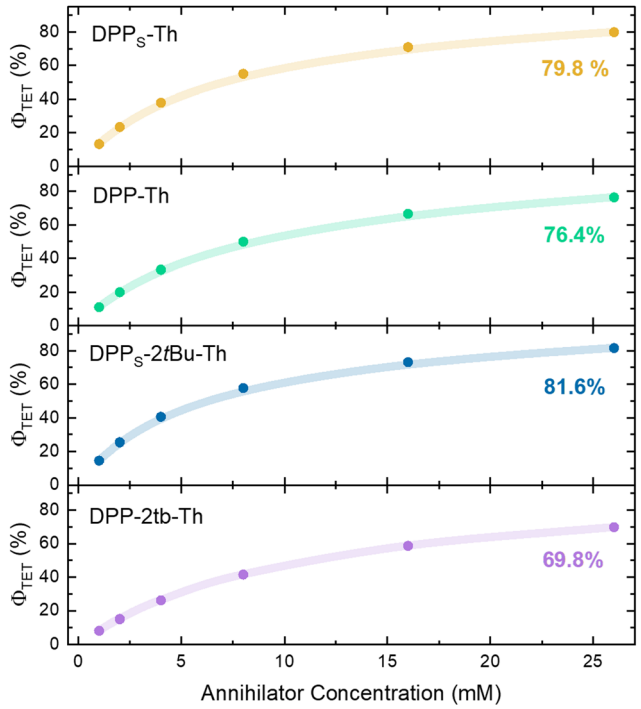

Fig. 5 Triplet energy transfer quantum yield (Φ_{TET}) dependence (dots) on annihilator concentration for the studied DPP:PdPc UC solutions in toluene. Line is shown as a guide for an eye. PdPc concentration was maintained at 30 μM for all measurements.

Φ_{TET} exhibited an upward trend with increasing annihilator concentration, demonstrating the importance of high annihilator concentrations in TTA-UC systems (Fig. 5).

The strapped compounds (**DPP$_S$-Th** and **DPP$_S$-2*t*Bu-Th**) exhibited slightly higher Φ_{TET} (79.8% and 81.6%) than the unstrapped **DPP-Th** and **DPP-2*t*Bu-Th** (Table 1 and Fig. 5). This may be explained by the strap moiety exposing one face of the DPP core, facilitating TET between PdPc sensitizer and DPP annihilators by reducing steric interactions.

Statistical probability factor

After the evaluation of TTA-UC parameters, the f factors for the DPP compounds were calculated according to eqn (1) (Table 1). **DPP$_S$-Th** exhibited the highest f value (25.2%) among the studied annihilators, limiting the $\Phi^{\infty}_{UC,g}$ to 12.6% if all other processes would approach unity. The strapped **DPP$_S$-Th** had a higher f value (25.2%) compared to its counterpart **DPP-Th** (22.9%) with ethyl-hexyl alkyl groups. The same pattern was seen between **DPP$_S$-2*t*Bu-Th** (15.2%) and **DPP-2*t*Bu-Th** (13.7%). Therefore, as the energy level distribution remains similar throughout the DPP annihilators, the increase in f values may be explained by a reduction in steric effects induced by the strapped alkyl groups. The exposure of one pi face could lead to enhanced non-radiative decay *via* aggregation or excimer formation. However, we do not observe significant differences in the line shape of emission of our DPPs at high *versus* low concentrations (Fig. S6, ESI†), implying the absence of aggregates or excimers. Additionally, the reduced distance between the core-to-core collisions for strapped DPPs may lead to increased TTA efficiency. Conversely, one of the factors that leads to smaller f values is bulky *t*Bu moieties which were previously thought to enhance UC performance of rubrene-based annihilators.[51,52] *t*Bu moieties have also previously been used to prevent the excimer formation in perylene derivatives,[48] however, this led to a decrease in effective annihilation radius hindering TTA. While *t*Bu groups can be used to increase the solubility of annihilators,[36] other alkyl moieties such as a strapped alkyl chains can be more beneficial both for solubility and TTA performance.

Generally, the strap functionalization and absence of bulky *t*Bu moieties on annihilator molecules lead to enhanced UC performance implying reduced steric interactions for higher f values. Thus, we demonstrate a general approach for optimizing annihilator performance *via* structural tuning of alkyl functionalities.

Conclusions

In this work, the impact of steric effects on the statistical probability factor (f) was investigated by synthesizing a series of alkyl functionalized DPP annihilators. As the excited state energy level distribution remained constant between these DPPs, the impact of steric effects and their influence on TTA-UC performance could be isolated. The strapped **DPP$_S$-Th** annihilator exhibited a high f value of 25.2%, as the elimination of bulky alkyl groups led to a reduction in steric interactions, optimizing the collisions required for efficient TTA-UC. The strap alkyl moiety was also demonstrated to increase Φ_{TET} and Φ_{TTA} *via* reduction of steric effects, thus enhancing the maximum achievable UC quantum yields ($\Phi^{\infty}_{UC,g}$). We demonstrated that the steric effects induced by the strap moiety are favorable for TTA-UC and that annihilator functionalization with unstrapped ethyl-hexyl chains or bulky *t*Bu groups should be avoided in the design of new annihilators. Therefore, we introduce a general strategy to minimize steric interactions and optimize annihilator performance, which will in turn further increase the widening application scope of TTA-UC.

Experimental

Full experimental details including synthesis and calculations are provided in the ESI.†

Author contributions

LN, SZ, and AP conceptualized the idea of this work. LN and SZ lead the experimental work. LN performed DFT calculations. LN, SZ, and AP performed chemical synthesis. LN and AP wrote the first draft of the manuscript as well as its revisions. All authors contributed to the analysis of the results.

Data availability

DFT calculation data have been deposited in a multi-disciplinary repository Zenodo. The raw calculation output files are provided for transparency and reproducibility. Data can be accessed *via* DOI: **https://doi.org/10.5281/zenodo.12692754**.

Conflicts of interest

There are no conflicts to declare.

Acknowledgements

This work was supported by start-up funds provided by the University of California San Diego. The authors acknowledge the use of facilities and instrumentation supported by NSF through the UC San Diego Materials Research Science and Engineering Center (UCSD MRSEC), grant # DMR-2011924. The authors acknowledge Keck Foundation for providing computational resources.

Notes and references

1 T. W. Schmidt and F. N. Castellano, *Phys. Chem. Lett.*, 2014, 4062–4072.
2 T. N. Singh-Rachford and F. N. Castellano, *Coord. Chem. Rev.*, 2010, **254**, 2560–2573.
3 P. Bharmoria, H. Bildirir and K. Moth-Poulsen, *Chem. Soc. Rev.*, 2020, **49**, 6529–6554.
4 M. Uji, T. J. B. Zähringer, C. Kerzig and N. Yanai, *Angew. Chem., Int. Ed.*, 2023, **62**, e202301506.
5 Y. Sasaki, S. Amemori, H. Kouno, N. Yanai and N. Kimizuka, *J. Mater. Chem. C*, 2017, **5**, 5063–5067.
6 A. Olesund, J. Johnsson, F. Edhborg, S. Ghasemi, K. Moth-Poulsen and B. Albinsson, *J. Am. Chem. Soc.*, 2022, **144**, 3706–3716.
7 C. Ye, V. Gray, J. Mårtensson and K. Börjesson, *J. Am. Chem. Soc.*, 2019, **141**, 9578–9584.
8 N. Nishimura, J. R. Allardice, J. Xiao, Q. Gu, V. Gray and A. Rao, *Chem. Sci.*, 2019, **10**, 4750–4760.
9 F. Auzel, *Chem. Rev.*, 2004, **104**, 139–174.
10 M. Mahboub, Z. Huang and M. L. Tang, *Nano Lett.*, 2016, **16**, 7169–7175.
11 N. Harada, Y. Sasaki, M. Hosoyamada, N. Kimizuka and N. Yanai, *Angew. Chem., Int. Ed.*, 2021, **60**, 142–147.
12 Y. Nakadai, S. Tsuchiya, M. Uehara, S. Umezawa, R. Motoki, H. Umezawa, T. Ikoma and T. Yui, *J. Phys. Chem. B*, 2022, **126**, 8245–8250.
13 M. Yang, S. Sheykhi, Y. Zhang, C. Milsmann and F. N. Castellano, *Chem. Sci.*, 2021, **12**, 9069–9077.
14 N. A. Durandin, J. Isokuortti, A. Efimov, E. Vuorimaa-Laukkanen, N. V. Tkachenko and T. Laaksonen, *J. Phys. Chem. C*, 2019, **123**, 22865–22872.
15 B. D. Ravetz, A. B. Pun, E. M. Churchill, D. N. Congreve, T. Rovis and L. M. Campos, *Nature*, 2019, **565**, 343–346.
16 Q. Liu, M. Xu, T. Yang, B. Tian, X. Zhang and F. Li, *ACS Appl. Mater. Interfaces*, 2018, **10**, 9883–9888.
17 Y. Sasaki, M. Oshikawa, P. Bharmoria, H. Kouno, A. Hayashi-Takagi, M. Sato, I. Ajioka, N. Yanai and N. Kimizuka, *Angew. Chem., Int. Ed.*, 2019, **58**, 17827–17833.
18 S. N. Sanders, T. H. Schloemer, M. K. Gangishetty, D. Anderson, M. Seitz, A. O. Gallegos, R. C. Stokes and D. N. Congreve, *Nature*, 2022, **604**, 474–478.
19 D. K. Limberg, J. H. Kang and R. C. Hayward, *J. Am. Chem. Soc.*, 2022, **144**, 5226–5232.
20 A. J. Carrod, V. Gray and K. Börjesson, *Energy Environ. Sci.*, 2022, **15**, 4982–5016.
21 T. J. B. Zähringer, J. A. Moghtader, M.-S. Bertrams, B. Roy, M. Uji, N. Yanai and C. Kerzig, *Angew. Chem., Int. Ed.*, 2023, **62**, e202215340.
22 T. Schloemer, P. Narayanan, Q. Zhou, E. Belliveau, M. Seitz and D. N. Congreve, *ACS Nano*, 2023, **4**, 3259–3288.
23 D. K. Limberg, J. H. Kang and R. C. Hayward, *J. Am. Chem. Soc.*, 2022, **144**, 5226–5232.
24 A. J. Carrod, V. Gray and K. Börjesson, *Energy Environ. Sci.*, 2022, **15**, 4982–5016.
25 D. G. Bossanyi, Y. Sasaki, S. Wang, D. Chekulaev, N. Kimizuka, N. Yanai and J. Clark, *JACS Au*, 2021, **1**, 2188–2201.
26 P. Baronas, G. Kreiza, L. Naimovičius, E. Radiunas, K. Kazlauskas, E. Orentas and S. Juršėnas, *J. Phys. Chem. C*, 2022, **126**, 15327–15335.
27 L. Naimovičius, E. Radiunas, M. Dapkevičius, P. Bharmoria, K. Moth-Poulsen and K. Kazlauskas, *J. Mater. Chem. C*, 2023, **11**, 14826–14832.
28 V. Gray, A. Dreos, P. Erhart, B. Albinsson, K. Moth-Poulsen and M. Abrahamsson, *Phys. Chem. Chem. Phys.*, 2017, **19**, 10931–10939.
29 S. N. Sanders, A. B. Pun, K. R. Parenti, E. Kumarasamy, L. M. Yablon, M. Y. Sfeir and L. M. Campos, *Chem*, 2019, **5**, 1988–2005.
30 L. Naimovičius, P. Bharmoria and K. Moth-Poulsen, *Mater. Chem. Front.*, 2023, **7**, 2297–2315.
31 J. B. Birks, *Phys. Lett. A*, 1967, **24**, 479–480.
32 A. Olesund, V. Gray, J. Mårtensson and B. Albinsson, *J. Am. Chem. Soc.*, 2021, **143**, 5745–5754.
33 S. Raišys, S. Juršėnas and K. Kazlauskas, *Solar RRL*, 2022, **6**, 1–9.
34 Q. Zhou, M. Zhou, Y. Wei, X. Zhou, S. Liu, S. Zhang and B. Zhang, *Phys. Chem. Chem. Phys.*, 2017, **19**, 1516–1525.
35 E. Radiunas, L. Naimovičius, S. Raišys, A. Jozeliūnaitė, E. Orentas and K. Kazlauskas, *J. Mater. Chem. C*, 2022, **10**, 6314–6322.
36 E. Radiunas, S. Raišys, S. Juršenas, A. Jozeliunaite, T. Javorskis, U. Šinkeviciute, E. Orentas and K. Kazlauskas, *J. Mater. Chem. C*, 2020, **8**, 5525–5534.
37 X. Wang and N. Marom, *Mol. Syst. Des. Eng.*, 2022, **1**, 11–13.
38 X. Wang, R. Tom, X. Liu, D. N. Congreve and N. Marom, *J. Mater. Chem. C*, 2020, **8**, 10816–10824.
39 J. Jortner, *Pure Appl. Chem.*, 1971, **27**, 389–420.
40 L. Naimovičius, E. Radiunas, B. Chatinovska, A. Jozeliūnaitė, E. Orentas and K. Kazlauskas, *J. Mater. Chem. C*, 2023, **11**, 698–704.

41 A. Olesund, S. Ghasemi, K. Moth-Poulsen and B. Albinsson, *J. Am. Chem. Soc.*, 2023, **145**, 22168–22175.
42 T. N. Singh-Rachford and F. N. Castellano, *J. Phys. Chem. A*, 2008, **112**, 3550–3556.
43 A. B. Pun, L. M. Campos and D. N. Congreve, *J. Am. Chem. Soc.*, 2019, **141**, 3777–3781.
44 S. Hoseinkhani, R. Tubino, F. Meinardi and A. Monguzzi, *Phys. Chem. Chem. Phys.*, 2015, **17**, 4020–4024.
45 N. Yanai, K. Suzuki, T. Ogawa, Y. Sasaki, N. Harada and N. Kimizuka, *J. Phys. Chem. A*, 2019, **123**, 10197–10203.
46 A. Lyons, L. Naimovičius, S. K. Zhang and A. B. Pun, *Angew. Chem., Int. Ed.*, 2024, e202411003.
47 F. Edhborg, H. Bildirir, P. Bharmoria, K. Moth-Poulsen and B. Albinsson, *J. Phys. Chem. B*, 2021, **125**, 6255–6263.
48 C. Ye, V. Gray, K. Kushwaha, S. Kumar Singh, P. Erhart and K. Börjesson, *Phys. Chem. Chem. Phys.*, 2020, **22**, 1715–1720.
49 Y. Murakami and K. Kamada, *Phys. Chem. Chem. Phys.*, 2021, **23**, 18268–18282.
50 B. D. Rihter, M. E. Kenney, W. E. Ford and M. A. J. Rodgers, *J. Am. Chem. Soc.*, 1990, **112**, 8064–8070.
51 A. Sawa, S. Shimada, N. Tripathi, C. Heck, H. Tachibana, E. Koyama, T. Mizokuro, Y. Hirao, T. Kubo, N. Tamai, D. Kuzuhara, H. Yamada and K. Kamada, *J. Mater. Chem. C*, 2023, **11**, 8502–8513.
52 E. Radiunas, M. Dapkevičius, S. Raišys, S. Juršenas, A. Jozeliunaite, T. Javorskis, U. Šinkevičiute, E. Orentas and K. Kazlauskas, *Phys. Chem. Chem. Phys.*, 2020, **22**, 7392–7403.